

# Anisotropic mass ejection from black hole-neutron star binaries: Diversity of electromagnetic counterparts

Koutarou Kyutoku<sup>1</sup>, Kunihito Ioka<sup>2</sup>, Masaru Shibata<sup>3</sup>

<sup>1</sup>*Department of Physics, University of Wisconsin-Milwaukee,  
P.O. Box 413, Milwaukee, Wisconsin 53201, USA*

<sup>2</sup>*Theory Center, Institute of Particles and Nuclear Studies,  
KEK, Tsukuba 305-0801, Japan*

<sup>3</sup>*Yukawa Institute for Theoretical Physics,  
Kyoto University, Kyoto 606-8502, Japan*

(Dated: September 3, 2018)

The merger of black hole-neutron star binaries can eject substantial material with the mass  $\sim 0.01\text{--}0.1M_\odot$  when the neutron star is disrupted prior to the merger. The ejecta shows significant anisotropy, and travels in a particular direction with the bulk velocity  $\sim 0.2c$ . This is drastically different from the binary neutron star merger, for which ejecta is nearly isotropic. Anisotropic ejecta brings electromagnetic-counterpart diversity which is unique to black hole-neutron star binaries, such as viewing-angle dependence, polarization, and proper motion. The kick velocity of the black hole, gravitational-wave memory emission, and cosmic-ray acceleration are also discussed.

PACS numbers: 04.25.D-, 04.30.Tv, 04.40.Dg

## I. INTRODUCTION

Black hole (BH)-neutron star (NS) binary coalescences are among the prime sources of gravitational waves (GWs) for ground-based detectors, such as Advanced LIGO, Advanced Virgo, and KAGRA [1–3]. Gravitational waves from BH-NS binaries will enable us to probe the supranuclear-density matter [4, 5] and cosmological expansion [6] via the NS tidal effect even without electromagnetic (EM) observation. The imprint of the NS tidal effect is the most prominent when the NS is disrupted outside the BH innermost stable circular orbit [7, 8]. If tidal disruption occurs outside it, a hot and massive remnant disk may be formed around a remnant BH. Such a system could drive an ultra-relativistic jet; therefore, BH-NS binaries are also important as possible progenitors of short-hard gamma-ray bursts (GRBs) [9].

Mass ejection from the BH-NS merger also has a long history of theoretical investigation [10], and has recently been getting a lot more attention. One of the most important reasons is the pressing necessity to understand EM radiation from, or EM counterparts to, the BH-NS merger. A variety of EM counterparts will be accompanied by the mass ejection from the merger of binary compact objects including NSs [11, 12]. Simultaneous detection of EM radiation with GWs are indispensable for confident GW detection and accurate localization of the GW sources [13].

In this paper, we explore possible signatures of mass ejection from the BH-NS merger based on our recent numerical-relativity simulations. Numerical relativity is a unique tool to understand the merger of binary compact objects. The numerical relativity community has been focusing primarily on GW emission and disk formation for the BH-NS merger (see [14] for reviews) and is just beginning to explore mass ejection from the BH-

NS merger [8, 15–17]. While characteristic properties of ejecta such as the mass and energy are reported in these works, observational implication of the ejecta is not fully understood yet. In particular, ejecta from the BH-NS merger shows significant anisotropy, and thus EM counterparts could show significant differences from ones by nearly isotropic ejecta from the NS-NS merger [18, 19].

## II. SIMULATION

Our BH-NS models are chosen so that the mass ratio, BH spin, and NS equation of state (EOS) are systematically varied. We fix the NS mass,  $M_{\text{NS}}$ , to be a representative value  $1.35M_\odot$  of observed NS-NS binaries [20]. The mass ratio of the BH to NS,  $Q$ , is varied from 3 to 7, where  $Q \gtrsim 5$  may correspond to a typical BH mass in low-mass x-ray binaries [21]. The nondimensional spin parameter of the BH (the spin divided by the mass squared),  $\chi$ , is chosen between 0 and 0.75. In this study, we focus on cases in which the BH spin is aligned with the orbital angular momentum. The NS EOS are modeled by the same piecewise polytropes as those adopted in [18], i.e., APR4, ALF2, H4, and MS1 (see also [22]). For these EOSs, radii of a  $1.35M_\odot$  NS span a wide range. Specifically, APR4, ALF2, H4, and MS1 give 11.1km, 12.4km, 13.6km, and 14.4km, respectively. Methods for computing initial conditions are described in [8, 23].

Our simulations are performed in full general relativity with an adaptive-mesh-refinement code, SACRA [24]. Improvements to previous simulations are summarized as follows (see also [18]). First, we extend computational domains so that we can track long-term evolution of ejecta. Specifically, we solve hydrodynamics equations within the edge length of  $\sim 1500$  km, and thus we can

TABLE I. Important values of representative models measured at 10 ms after the onset of the merger for highest resolution runs.  $M_{\text{disk}}$  and  $M_{\text{ej}}$  are the bound and unbound masses, respectively, outside the apparent horizon of the BH.  $T_{\text{ej}}$  is the kinetic energy of the ejecta, and  $v_{\text{ej}}$  is the bulk velocity of the ejecta.

$Q$	$\chi$	EOS	$M_{\text{disk}}[M_{\odot}]$	$M_{\text{ej}}[M_{\odot}]$	$T_{\text{ej}}$ (erg)	$v_{\text{ej}}[c]$
3	0.75	APR4	0.18	0.01	$5 \times 10^{50}$	0.19
3	0.75	ALF2	0.23	0.05	$3 \times 10^{51}$	0.21
3	0.75	H4	0.29	0.05	$2 \times 10^{51}$	0.20
3	0.75	MS1	0.29	0.07	$4 \times 10^{51}$	0.21
3	0	MS1	0.14	0.02	$8 \times 10^{50}$	0.19
5	0.75	H4	0.27	0.05	$3 \times 10^{51}$	0.22
7	0.75	H4	0.16	0.04	$3 \times 10^{51}$	0.19

track ejecta motion up to  $\sim 10$  ms taking the fact that the ejecta velocity is usually smaller than  $0.5c$ , where  $c$  is the speed of light. Asymptotic properties such as the velocity and kinetic energy would not be correctly estimated if we measure them in a near zone. Hence, the large computational domain is essential for an accurate study of the ejecta. Second, we decrease the density of artificial atmosphere, which is inevitable in conservative hydrodynamics schemes. The atmospheric density is at most  $10^3 \text{ g cm}^{-3}$ , and negligible for ejecta (see Fig. 1). Indeed, we confirmed that ejecta properties depend very weakly on the atmospheric density as far as it is sufficiently low. Specifically, varying the atmospheric density by an order of magnitude changes the ejecta properties only by 10%-20%. Finally, we improve grid resolutions by  $\sim 20\%$  so that the NS radius is covered by  $\approx 50$  grid points in the highest resolution runs. The radius of the ejecta is always covered by  $\approx 50$ -60 grid points in the equatorial plane, and  $\approx 10$  grid points in the perpendicular direction (see the next section). We perform simulations with 3 different resolutions for selected models, and estimate that ejecta properties are accurate within  $\approx 10\%$  for many cases and within a factor of 2 for the worst cases in which the ejecta mass is small. This accuracy is sufficient for the purpose of this article, which mainly discuss qualitative signatures. A convergence study will be presented in a separate paper with detailed discussions of our systematic simulations.

### III. MASS EJECTION

When the NS is disrupted by the BH tidal field, a one-armed spiral structure called the tidal tail is formed around the BH. Although a large part of the tail eventually falls back onto the remnant disk and BH, its outermost part obtains a sufficient angular momentum and kinetic energy to become unbound via hydrodynamic angular momentum transport processes. Dynamical mass ejection from the BH-NS merger is driven dominantly by this tidal effect. We also find that some material in the

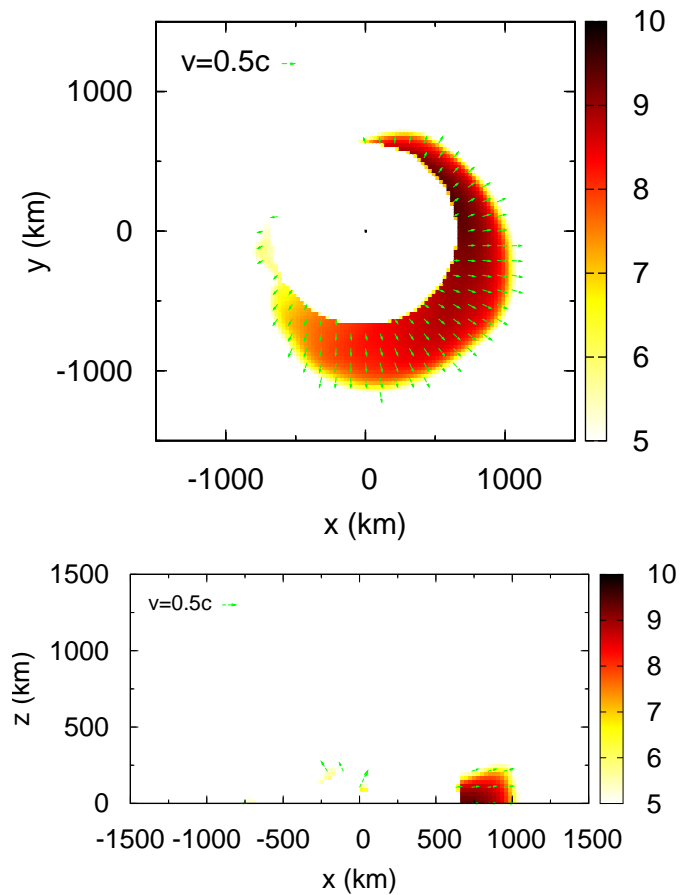


FIG. 1. The rest-mass density ( $\rho$ ) profiles of ejecta overplotted with the velocity at  $\approx 10$  ms after the merger for  $Q = 5$ ,  $\chi = 0.75$ , and H4 EOS model. We only show unbound material to elucidate geometry of the ejecta, and the blank region between the ejecta and BH is filled with unshown bound material. The top and bottom panels are for the  $xy$ - and  $xz$ -planes, respectively. The color panel on the right of each plot is  $\log_{10} \rho$  in  $\text{g cm}^{-3}$ . The region above  $\sim 500$  km in the bottom panel is much clearer than that in a typical NS-NS merger (see the corresponding panels of Figs. 3-5 in [18]).

vicinity of the BH becomes unbound when the tidal tail hits itself as it spirals around the BH. This ejection may be ascribed to the shock heating, but this shock-driven component is always subdominant.

Ejecta exhibits a crescentlike shape as depicted in Fig. 1 in most cases. Specifically, a typical opening angle of the ejecta in the equatorial plane is  $\varphi_{\text{ej}} \approx \pi$ . Such a nonaxisymmetric shape arises because the sound-crossing time scale is shorter than the orbital period at the onset of tidal disruption. Furthermore, ejecta spreads dominantly in the equatorial plane, and expands only slowly in the direction perpendicular to the equatorial plane (hereafter, the  $z$ -direction). The reason for this is that the ejection is driven mainly by the tidal effect, which is most efficient in the equatorial plane. Thus, a portion of circumferential material will be subsequently swept by the ejecta. A typical half opening angle of the ejecta

around the equatorial plane is  $\theta_{\text{ej}} \approx 1/5$  radian; and, this implies that the ejecta velocity in the equatorial plane  $v_{\parallel}$  is larger by a factor of  $1/\theta_{\text{ej}} \approx 5$  than that in the  $z$ -direction  $v_{\perp}$ . Here,  $v_{\parallel}$  may be identified with the radial velocity, and the azimuthal velocity should become negligible soon after the ejection due to the angular momentum conservation. Indeed, azimuthal velocity is very small in Fig. 1. Aside from the ejecta itself, the region above the remnant BH is much clearer than that for the NS-NS merger, and thus the baryon-loading problem of GRB jets may be less severe.

The ejecta mass  $M_{\text{ej}}$  depends on binary parameters and NS EOSs and are typically in the range of  $\sim 0.01$ – $0.1M_{\odot}$  when the tidal disruption occurs and the disk mass  $M_{\text{disk}}$  exceeds  $\sim 0.1M_{\odot}$ . Important values are shown in Table I for representative models in which  $M_{\text{disk}} \gtrsim 0.1M_{\odot}$ . The value of  $M_{\text{ej}}$  is generally large when the NS EOS is stiff and the NS radius is large for fixed values of  $Q$  and  $\chi$ , because the mass ejection is driven primarily by the tidal effect. This dependence on the NS EOS and radius is opposite to the case of the NS-NS merger in general relativity, where rapid rotation and oscillation of a remnant massive NS drive ejection [18, 19]. We speculate that ejecta from the BH-NS merger might account for a substantial portion of the  $r$ -process nucleosynthesis (see also below) compared to that from the NS-NS merger if the realistic NS EOS is stiff, and vice versa. When the NS is not disrupted prior to the merger, the ejecta mass is negligible for current astrophysical interest. The ejecta mass is always smaller than the disk mass, and a relation  $M_{\text{ej}} \approx 0.05$ – $0.25M_{\text{disk}}$  approximately holds for a wide range. When the disk and ejecta are very massive, it seems that  $M_{\text{ej}}$  can be a larger fraction of  $M_{\text{disk}}$  than this relation indicates.

The ejecta from the BH-NS merger has a bulk linear momentum,  $P_{\text{ej}}$ , and resulting large bulk velocity  $v_{\text{ej}} \equiv P_{\text{ej}}/M_{\text{ej}} \sim 0.2c$ , in a particular direction. These bulk linear momentum and velocity would essentially vanish for nearly spherical ejecta such as one from the NS-NS merger. The value of  $v_{\text{ej}} \sim 0.2c$  depends only weakly on the binary parameters and NS EOS as far as the mass ejection is substantial.

Typical values of kinetic energy  $T_{\text{ej}}$  are in the range  $\sim 5 \times 10^{50}$ – $5 \times 10^{51}$  erg. The average velocity of the ejecta  $v_{\text{ave}} \approx (2T_{\text{ej}}/M_{\text{ej}})^{1/2}$  is typically  $0.25$ – $0.3c$  and is naturally larger than  $v_{\text{ej}}$ . The contribution of  $v_{\perp}$  to  $T_{\text{ej}}$  is smaller by a factor of  $\theta_{\text{ej}}^2$  than that of  $v_{\parallel}$ , and thus a relation  $v_{\text{ave}} \approx v_{\parallel}$  holds. For an axisymmetric outflow truncated at an opening angle  $\varphi_{\text{ej}}$ , a relation  $v_{\text{ej}}/v_{\parallel} \approx \sin(\varphi_{\text{ej}}/2)/(\varphi_{\text{ej}}/2)$  should hold, and thus the ejecta opening angle in the equatorial plane is estimated to be  $\varphi_{\text{ej}} \approx (0.7$ – $1.3)\pi$  radian. This is consistent with Fig. 1.

## IV. DISCUSSION

In this section, we discuss possible consequences of the anisotropic ejecta from the BH-NS merger in chronological order as closely as possible. For convenience, we introduce  $M_{1.35} \equiv M_{\text{NS}}/1.35M_{\odot}$ ,  $A_5 \equiv (1+Q)/(1+5)$ ,  $M_{\text{ej},0.03} \equiv M_{\text{ej}}/0.03M_{\odot}$ ,  $v_{\text{ej},0.2} \equiv v_{\text{ej}}/0.2c$ ,  $v_{\text{ave},0.3} \equiv v_{\text{ave}}/0.3c$ ,  $\theta_{\text{ej},i} \equiv \theta_{\text{ej}}/(1/5)$ , and  $\varphi_{\text{ej},i} \equiv \varphi_{\text{ej}}/\pi$ .

### A. Kick velocity of the black hole

The remnant BH should receive backreaction from the ejecta with  $M_{\text{ej}}$  and  $v_{\text{ej}}$ , and obtain substantial “ejecta kick” velocity [25]. The total mass of the remnant BH and surrounding disk is determined approximately by the mass of the binary at infinite separation  $m_0 = (1+Q)M_{\text{NS}}$ , neglecting  $M_{\text{ej}}$  and energy carried by GWs  $\approx 0.05m_0c^2$ . Thus, the ejecta kick velocity of the remnant BH-disk will be

$$v_{\text{kick}} \approx \frac{M_{\text{ej}}}{m_0} v_{\text{ej}} = 220 \text{ km s}^{-1} M_{\text{ej},0.03} v_{\text{ej},0.2} M_{1.35}^{-1} A_5^{-1}. \quad (1)$$

This value is larger than escape velocity of globular clusters and dwarf galaxies for many cases, and can exceed that of small galaxies under suitable conditions [26].

The ejecta kick velocity,  $v_{\text{kick}}$ , can be larger than the kick velocity due to GW radiation reaction. Specifically, the GW kick velocity is at most  $\sim 150 \text{ km s}^{-1}$  when the NS is disrupted prior to the merger, even if the BH spin is misaligned [8, 15, 27, 28]. The reason for this is that the linear momentum is radiated most efficiently when the binary is about to merge, and, therefore, earlier disruption significantly suppresses the GW kick velocity. Thus, the ejecta kick velocity can dominate the velocity of the remnant when tidal disruption is prominent.

### B. Gravitational-wave memory

Because the ejecta and remnant BH-disk travel in the opposite direction after the merger, nonoscillatory GW emission, i.e., GW memory, is expected. Assuming that the remnant mass  $\approx m_0$  is much larger than  $M_{\text{ej}}$ , magnitude of this (linear) ejecta memory is given approximately by [29]

$$\delta h \approx \frac{2GM_{\text{ej}}v_{\text{ej}}^2}{c^4 D} = 1.1 \times 10^{-24} M_{\text{ej},0.03} v_{\text{ej},0.2}^2 D_2^{-1}, \quad (2)$$

where  $G$  is the gravitational constant and  $D \equiv D_2 \times 100$  Mpc is a distance from the binary to the observer. Taking the fact that the expected rise time of ejecta memory is much shorter than the inverse of frequency at which ground-based detectors are most sensitive, ( $\sim 100 \text{ Hz}$ ) $^{-1}$ , it may be possible to detect ejecta memory by the Einstein Telescope [30] if the ejecta is as massive as  $\gtrsim 0.1M_{\odot}$ .

A possibility of such significant mass ejection is not negligible if the BH spin can be very large [16].

The ejecta memory as well as GWs from the binary coalescence can be strongest in the  $z$ -direction. Such memory would easily be distinguished from linear memory from GRB jets [31] and nonlinear memory from coalescence GWs [32], which are very weak in the  $z$ -direction, if we observe the binary from this direction.

### C. Macronova/kilonova

The macronova a.k.a. kilonova is quasithermal radiation from the ejecta heated by the radioactive decay of  $r$ -process elements [33–35]. Although properties of  $r$ -process elements such as opacities are still uncertain so that accurate predictions are difficult [36, 37], the macronova/kilonova is one of the most promising EM counterparts to the BH-NS merger.

Peak values of the macronova/kilonova are estimated when the diffusion time scale becomes equal to the dynamical time scale, which is essentially the time after the merger. Assuming random walks of photons in spherical ejecta, the peak time is estimated to be  $t_{\text{peak},s} \approx (3\kappa M_{\text{ej}}/4\pi c v_{\text{ave}})^{1/2} = 8 \text{ day } \kappa_1^{1/2} M_{\text{ej},0.03}^{1/2} v_{\text{ave},0.3}^{-1/2}$ , where  $\kappa \equiv \kappa_1 \times 10 \text{ g}^{-1} \text{ cm}^2$  is the opacity. If a fraction  $f \equiv f_{-6} \times 10^{-6}$  of  $M_{\text{ej}}c^2$  is radiated, the peak luminosity is expected to be  $L_{\text{peak},s} \approx f M_{\text{ej}}c^2/t_{\text{peak},s} = 7 \times 10^{40} \text{ erg s}^{-1} f_{-6} \kappa_1^{-1/2} M_{\text{ej},0.03}^{1/2} v_{\text{ej},0.3}^{1/2}$ , and the temperature at the peak is  $T_{\text{peak},s} \approx (L_{\text{peak},s}/4\pi v_{\text{ave}}^2 t_{\text{peak},s}^2 \sigma)^{1/4} = 1200 \text{ K } f_{-6}^{1/4} \kappa_1^{-3/8} M_{\text{ej},0.03}^{-1/8} v_{\text{ej},0.3}^{-1/8}$ , where  $\sigma$  is the Stefan-Boltzmann constant.

The emission could be modified by ejecta geometry for the BH-NS merger. We approximate ejecta geometry by an axisymmetric cylinder with  $v_{\parallel}$  and  $v_{\perp}$  in the radial and  $z$ -directions, respectively, and truncate at an opening angle  $\varphi_{\text{ej}}$ . Assuming that photons escape from the  $z$ -direction due to a short distance, the peak time is estimated as

$$t_{\text{peak}} \approx \left( \frac{\kappa M_{\text{ej}} v_{\perp}}{c \varphi_{\text{ej}} v_{\parallel}^2} \right)^{1/2} = 4 \text{ day } \kappa_1^{1/2} M_{\text{ej},0.03}^{1/2} v_{\text{ave},0.3}^{-1/2} \theta_{\text{ej},i}^{1/2} \varphi_{\text{ej},i}^{-1/2}. \quad (3)$$

Accordingly, the peak luminosity is

$$L_{\text{peak}} \approx \frac{f M_{\text{ej}} c^2}{t_{\text{peak}}} = 1.4 \times 10^{41} \text{ erg } f_{-6} \kappa_1^{-1/2} M_{\text{ej},0.03}^{1/2} v_{\text{ej},0.3}^{1/2} \theta_{\text{ej},i}^{-1/2} \varphi_{\text{ej},i}^{1/2}, \quad (4)$$

and finally the temperature at the peak is

$$T_{\text{peak}} \approx \left( \frac{L_{\text{peak}}}{\varphi_{\text{ej}} v_{\parallel}^2 t_{\text{peak}}^2 \sigma} \right)^{1/4} = 3000 \text{ K } f_{-6}^{1/4} \kappa_1^{-3/8} M_{\text{ej},0.03}^{-1/8} v_{\text{ave},0.3}^{-1/8} \theta_{\text{ej},i}^{-3/8} \varphi_{\text{ej},i}^{1/8}. \quad (5)$$

These rough estimates suggest that characteristics of the macronova/kilonova associated with anisotropic ejecta from the BH-NS merger will be modified by a factor of a few compared to those associated with the isotropic one from the NS-NS merger when the values of the ejecta mass and velocity are the same.

Directional dependence is important for the macronova/kilonova of the BH-NS merger [38]. In particular, the flux will differ by a factor of  $\approx 1/\theta_{\text{ej}} \approx 5$  for different viewing angles at  $t_{\text{peak}}$ . Specifically, the radiation will be dim if we are located in the equatorial plane. The time evolution of light curves will also differ, because the diffusion timescale is different for different viewing angles. Although atomic line structures of  $r$ -process elements will be blended due to the variety of elements and energy levels, observation might be possible from the  $z$  direction, for which the line broadening is not severe due to the small velocity,  $v_{\perp}$ , if some prominent lines are isolated. Blueshifts of lines are also small in the  $z$  direction. In addition, linear polarization up to  $\approx 4\%$ – $5\%$  is expected for an aspherical photosphere observed in the equatorial plane [39].

### D. Synchrotron radio flare

Blast waves will develop between the ejecta and interstellar medium (ISM) as the ejecta travels in the ISM. If electrons are accelerated to nonthermal velocity distribution and magnetic fields are amplified behind the blast waves in a similar manner to supernova remnants and GRB afterglows, synchrotron radio flares should arise [40]. The synchrotron radio flare is also one of the most promising EM counterparts.

The peak time of the flare is the time at which the ejecta accumulates the mass comparable to its own from the ISM with density  $n_{\text{H}} \equiv n_{\text{H},0} \times 1 \text{ cm}^{-3}$  and begins to be decelerated. The deceleration radius is given by  $R_{\text{dec},s} = (3M_{\text{ej}}/4\pi m_{\text{p}} n_{\text{H}})^{1/3} = 0.7 \text{ pc } M_{\text{ej},0.03}^{1/3} n_{\text{H},0}^{-1/3}$  for spherical ejecta, and thus the deceleration time is given by  $t_{\text{dec},s} = R_{\text{dec},s}/v_{\text{ave}} = 7 \text{ yr } M_{\text{ej},0.03}^{1/3} n_{\text{H},0}^{-1/3} v_{\text{ave},0.3}^{-1}$ .

The ejecta from the BH-NS merger is not spherical, and can accumulate only a small portion of the ISM within a fixed radius. Thus, the ejecta has to travel a longer distance  $R_{\text{dec}} > R_{\text{dec},s}$  to be decelerated than spherical ejecta. Here, we assume that values of  $v_{\parallel}$  and  $v_{\perp}$  do not change significantly before the deceleration. This would lead to constant values of  $\theta_{\text{ej}}$  and  $\varphi_{\text{ej}}$  before the deceleration, which is expected to occur at

$$R_{\text{dec}} \approx R_{\text{dec},s} \left( \frac{\pi/2}{\theta_{\text{ej}}} \right)^{1/3} \left( \frac{2\pi}{\varphi_{\text{ej}}} \right)^{1/3} = 1.7 \text{ pc } M_{\text{ej},0.03}^{1/3} n_{\text{H},0}^{-1/3} \theta_{\text{ej},i}^{-1/3} \varphi_{\text{ej},i}^{-1/3}, \quad (6)$$

and, therefore, the peak time is

$$t_{\text{dec}} = \frac{R_{\text{dec}}}{v_{\parallel}} = 18 \text{ yr } M_{\text{ej},0.03}^{1/3} v_{\text{ave},0.3}^{-1} n_{\text{H},0}^{-1/3} \theta_{\text{ej},i}^{-1/3} \varphi_{\text{ej},i}^{-1/3}. \quad (7)$$

The peak time should be closer to (but still longer than due to the energy conservation)  $t_{\text{dec},s}$  if the ejecta approaches a spherical state. The reality may exist between these two limits. We left precise modelings of geometry evolution for the future study.

The peak luminosity and flux of the flare do not depend on geometry as far as ejecta evolves adiabatically. The reason for this is that the peak time is still the time at which the ejecta accumulate  $M_{\text{ej}}$  from the ISM, and thus the number of emitting electrons and their characteristic frequency do not change. Directional dependence of the flare as well as that of the macronova/kilonova is worth studying.

### E. Proper motion of radio images

Because the ejecta moves with  $v_{\text{ej}}$ , radio observation will be able to detect the proper motion of radio images in the timescale of  $t_{\text{dec}}$  in addition to expansion of images. A characteristic travel distance may be given by  $R_{\text{dec}}(v_{\text{ej}}/v_{\text{ave}})$ . Averaging over random distribution of ejecta direction halves the projected distance. In reality, however, GW observation may be biased toward the  $z$  axis, and then the biased average could be larger. We expect the projected proper motion of radio images to be  $O(1)$  pc around the synchrotron radio flare peak. This implies that the radio image is expected to move  $O(1)$  mas for a BH-NS binary at  $O(100)$  Mpc. Current radio instruments may resolve this angle [41].

The proper motion will give us a way to distinguish the BH-NS merger from the NS-NS merger, because proper motion of radio images should be much smaller for the latter, whereas expansion of images should be common to two merger types. It is not easy to distinguish between BH-NS and NS-NS binaries only from GW observation, especially when the BH is less massive [42]. Thus, information provided by EM counterparts is also useful for the determination of merger types [43, 44].

### F. Cosmic-ray acceleration

Physical condition of the ejecta is expected to be similar to that of a supernova remnant. This implies that

the cosmic-ray (CR) acceleration will occur in the remnant of ejecta from the BH-NS merger via diffusive shock acceleration [45, 46], as well as the NS-NS merger. The maximum attainable energy of CRs is given by the Hillas condition  $\varepsilon_{\text{max}} = Ze\beta BR$  [47], where  $Z$ ,  $\beta$ ,  $B$ , and  $R$  are the proton number, shock velocity divided by  $c$ , magnetic field, and typical source size, respectively. Assuming that a fraction  $\epsilon_B \equiv \epsilon_{B,-1} \times 0.1$  of  $T_{\text{ej}}$  is converted to magnetic field energy, we obtain

$$\varepsilon_{\text{max}} = 2.4 \times 10^{18} \text{ eV } Z M_{\text{ej},0.03}^{1/3} v_{\text{ave},0.3}^2 \epsilon_{B,-1}^{1/2} n_{\text{H},0}^{1/6} \theta_{\text{ej},i}^{2/3} \varphi_{\text{ej},i}^{-1/3}, \quad (8)$$

where we adopt  $R = R_{\text{dec}}\theta_{\text{ej}}$ . The higher energy than that for supernova remnants primarily owes to the faster ejecta velocity.

Cosmic rays from the galactic BH-NS merger could explain observed CRs above the knee region up to the ankle region. Taking the fact that ejecta kinetic energy is comparable to that of supernova remnants and comparing galactic BH-NS merger rate estimation  $\sim 10^{-7}-10^{-4} \text{ yr}^{-1}$  [48] with the galactic supernova rate  $\sim 0.01 \text{ yr}^{-1}$ , the CR energy above the knee can be explained. Evidently, acceleration, propagation, and galactic confinement of CRs including nuclei have to be investigated in more detail.

Acceleration of heavy elements like irons to even an ultrahigh energy  $\gtrsim 10^{20} \text{ eV}$  are also possible for massive ejecta  $\gtrsim 0.2M_{\odot}$  such as the ones reported in [16]. Although an energetics constraint is not assuring, observed energy of ultrahigh energy CRs [49] is marginally consistent within the uncertainty of merger rate estimation. Assuming that a fraction  $\epsilon_{\text{CR}} \equiv \epsilon_{\text{CR},-1} \times 0.1$  of ejecta kinetic energy averaged over BH-NS binary distribution  $\langle T_{\text{ej}} \rangle \equiv \langle T_{\text{ej},51} \rangle \times 10^{51} \text{ erg}$  is converted to CR energy, the required merger rate is approximately  $\epsilon_{\text{CR},-1} \langle T_{\text{ej},51} \rangle^{-1} \text{ Mpc}^{-3} \text{ Myr}^{-1}$ , where  $1 \text{ Mpc}^{-3} \text{ Myr}^{-1}$  is the ‘‘high’’ estimation [48].

### ACKNOWLEDGMENTS

We are grateful to Alan G. Wiseman, Masaomi Tanaka, and Kenta Hotokezaka for valuable discussions. This work was supported by the Grant-in-Aid for Scientific Research Grants No. 21684014, No. 22244030, No. 24000004, No. 24103006, and No. 24740163 of Japanese MEXT, and by JSPS Postdoctoral Fellowship for Research Abroad.

---

[1] J. Abadie et al., Nucl. Instrum. Methods Phys. Res., Sect. A **624**, 223 (2010)  
 [2] T. Accadia et al., Class. Quant. Grav. **28**, 025005 (2011)  
 [3] K. Kuroda et al., Class. Quant. Grav. **27**, 084004 (2010)

[4] B. D. Lackey, K. Kyutoku, M. Shibata, P. R. Brady, and J. L. Friedman, Phys. Rev. D **85**, 044061 (2012)  
 [5] B. D. Lackey, K. Kyutoku, M. Shibata, P. R. Brady, and J. L. Friedman arXiv:1303.6298

- [6] C. Messenger and J. Read, *Phys. Rev. Lett.* **108**, 091101 (2012)
- [7] K. Kyutoku, M. Shibata, and K. Taniguchi, *Phys. Rev. D* **82**, 044049 (2010)
- [8] K. Kyutoku, H. Okawa, M. Shibata, and K. Taniguchi, *Phys. Rev. D* **84**, 064018 (2011)
- [9] R. Narayan, B. Paczyński, and T. Piran, *Astrophys. J.* **395**, L83 (1992)
- [10] J. M. Lattimer and D. N. Schramm, *Astrophys. J.* **192**, L145 (1974)
- [11] B. D. Metzger and E. Berger, *Astrophys. J.* **746**, 48 (2012)
- [12] T. Piran, E. Nakar, and S. Rosswog, *Mon. Not. Roy. Astron. Soc.* **430**, 2121 (2013)
- [13] S. Nissanke, M. Kasliwal, and A. Georgieva, *Astrophys. J.* **767**, 124 (2013)
- [14] M. Shibata and K. Taniguchi, *Living Rev. in Relativity* **14**, 6 (2011)
- [15] F. Foucart, M. B. Deaton, M. D. Duez, L. E. Kidder, I. MacDonald, C. D. Ott, H. P. Pfeiffer, M. A. Scheel, B. Szilágyi, and S. A. Teukolsky, *Phys. Rev. D* **87**, 084006 (2013)
- [16] G. Lovelace, M. D. Duez, F. Foucart, L. E. Kidder, H. P. Pfeiffer, M. A. Scheel, and B. Szilágyi, *Class. Quant. Grav.* **30**, 135004 (2013)
- [17] M. B. Deaton, M. D. Duez, F. Foucart, E. O'Connor, C. D. Ott, L. E. Kidder, C. D. Muhlberger, M. A. Scheel, and B. Szilágyi [arXiv:1304.3384](https://arxiv.org/abs/1304.3384)
- [18] K. Hotokezaka, K. Kiuchi, K. Kyutoku, H. Okawa, Y.-I. Sekiguchi, M. Shibata, and K. Taniguchi, *Phys. Rev. D* **87**, 024001 (2013)
- [19] A. Bauswein, S. Goriely, and H.-T. Janka, *Astrophys. J.* **773**, 78 (2013)
- [20] F. Özel, D. Psaltis, R. Narayan, and A. S. Villarreal, *Astrophys. J.* **757**, 55 (2012)
- [21] F. Özel, D. Psaltis, R. Narayan, and J. E. McClintock, *Astrophys. J.* **725**, 1918 (2010)
- [22] J. S. Read, B. D. Lackey, B. J. Owen, and J. L. Friedman, *Phys. Rev. D* **79**, 124032 (2009)
- [23] K. Kyutoku, M. Shibata, and K. Taniguchi, *Phys. Rev. D* **79**, 124018 (2009)
- [24] T. Yamamoto, M. Shibata, and K. Taniguchi, *Phys. Rev. D* **78**, 064054 (2008)
- [25] S. Rosswog, M. B. Davies, F. Thielemann, and T. Piran, *Astron. Astrophys.* **360**, 171 (2000)
- [26] D. Merritt, M. Milosavljević, M. Favata, S. A. Hughes, and D. E. Holz, *Astrophys. J.* **607**, L9 (2004)
- [27] M. Shibata, K. Kyutoku, T. Yamamoto, and K. Taniguchi, *Phys. Rev. D* **79**, 044030 (2009)
- [28] F. Foucart, M. D. Duez, L. E. Kidder, and S. A. Teukolsky, *Phys. Rev. D* **83**, 024005 (2011)
- [29] V. B. Braginsky and K. S. Thorne, *Nature (London)* **327**, 123 (1987)
- [30] B. Sathyaprakash et al., *Class. Quant. Grav.* **29**, 124013 (2012)
- [31] N. Sago, K. Ioka, T. Nakamura, and R. Yamazaki, *Phys. Rev. D* **70**, 104012 (2004)
- [32] M. Favara, *Class. Quant. Grav.* **27**, 084036 (2010)
- [33] L.-X. Li and B. Paczyński, *Astrophys. J.* **507**, L59 (1998)
- [34] S. R. Kurkarni [arXiv:astro-ph/0510256](https://arxiv.org/abs/astro-ph/0510256)
- [35] B. D. Metzger, G. Martínez-Pinedo, S. Darbha, E. Quataert, A. Arcones, D. Kasen, R. Thomas, P. Nugent, I. V. Panov, and N. T. Zinner, *Mon. Not. Roy. Astron. Soc.* **406**, 2650 (2010)
- [36] J. Barnes and D. Kasen [arXiv:1303.5787](https://arxiv.org/abs/1303.5787)
- [37] D. Kasen, N. R. Badnell, and J. Barnes [arXiv:1303.5788](https://arxiv.org/abs/1303.5788)
- [38] M. Tanaka, K. S. Kawabata, T. Hattori, P. A. Mazzali, K. Aoki, M. Iye, K. Maeda, K. Nomoto, E. Pian, T. Sasaki, and M. Yamanaka, *Astrophys. J.* **754**, 63 (2012)
- [39] P. Höflich, *Astron. Astrophys.* **246**, 481 (1991)
- [40] E. Nakar and T. Piran, *Nature (London)* **478**, 82 (2011)
- [41] G. B. Taylor, D. A. Frail, E. Berger, and S. R. Kulkarni, *Astrophys. J.* **609**, L1 (2004)
- [42] M. Hannam, D. A. Brown, S. Fairhurst, C. L. Fryer, and I. W. Harry, *Astrophys. J.* **766**, L14 (2013)
- [43] N. Stone, A. Loeb, and E. Berger, *Phys. Rev. D* **87**, 084053 (2013)
- [44] K. Kyutoku, K. Ioka, and M. Shibata [arXiv:1209.5747](https://arxiv.org/abs/1209.5747)
- [45] A. R. Bell, *Mon. Not. Roy. Astron. Soc.* **182**, 147 (1978)
- [46] R. D. Blandford and J. P. Ostriker, *Astrophys. J.* **221**, L29 (1978)
- [47] A. M. Hillas, *Ann. Rev. Astron. Astrophys.* **22**, 425 (1984)
- [48] J. Abadie et al., *Class. Quant. Grav.* **27**, 173001 (2010)
- [49] K. Murase and H. Takami, *Astrophys. J.* **690**, L14 (2009)